

Automatic Detection of Region-Mura Defects in TFT-LCD

Based on Regression Diagnostics

Yu-Chiang Chuang^{† 1} and Shu-Kai S. Fan²

Department of Industrial Engineering and Management,
Yuan Ze University, Tao Yuan County, Taiwan 320, (ROC)

Email: jack@r2r.iem.yzu.edu.tw¹
simonfan@saturn.yzu.edu.tw²

Abstract. In recent days, large-sized flat-panel display (FPD) has been increasingly applied to computer monitors and TVs. Mura defects, appearing as low contrast or non-uniform brightness region, sometimes occur in manufacturing of the Thin-Film Transistor Liquid-Crystal Displays (TFT-LCD). Implementation of automatic Mura inspection methods is necessary for TFT-LCD production. Various existing Mura detection methods based on regression diagnostics, surface fitting and data transformation have been presented with good performance. This paper proposes an efficient Mura detection method that is based on a regression diagnostics using studentized residuals for automatic Mura inspection of FPD. The input image is estimated by linear model and then the studentized residuals are calculated for filtering Mura region. After image dilation, the proposed threshold is determined for detecting the non-uniform brightness region in TFT-LCD by means of monitoring the every pixel in the image. The experimental results obtained from several test images are used to illustrate the effectiveness and efficiency of the proposed method for Mura detection.

Keywords: Mura defect, regression analysis, TFT-LCD manufacturing, studentized residuals

1. INTRODUCTION

Large-sized TFT-LCD (Thin Film Transistor Liquid Crystal Display) devices have been applied to many applications in recent years. To assure the product quality and improve the competitiveness in the field of the TFT-LCD display, one of the most important processes is to visually inspect potential defects which might occur during in TFT-LCD manufacturing. The most common defect inspection is done by human visual inspection, but it cannot generate stable inspection outputs due to restrictions of human vision and human subjectivity. In addition, some defects are not easy to be detected by human-eye inspection especially in large-sized TFT-LCD. Therefore, Automatic Mura defect detection becomes a critical task to maintain quality and reduce production cost in LCD manufacturing.

Mura defects appear as low contrast, non-uniform brightness regions in TFT-LCD, and they are larger than one pixel in usual (Pratt et al. 1998). In Figure 1, there are several types of Mura defects in the TFT-LCD, and they are defined as spot-Mura, line-Mura and region-Mura, respectively. Those defects are not easy to be detected by human inspection or simple threshold method due to the human subjectivity and non-uniform illumination

conditions. In this paper, the automatic inspection method is proposed for detecting the Mura defect in TFT-LCD.

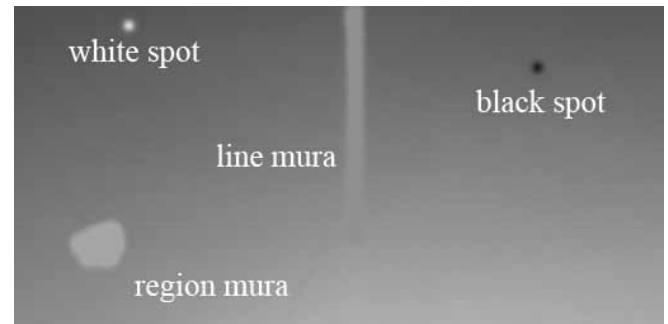


Figure 1: Illustration of line, spot and region Mura.

Several algorithms have been proposed for detecting Mura defects on TFT-LCD. Lu and Tsai (2008) proposed a new image reconstruction procedure using independent component analysis (ICA). ICA is used to determine the de-mixing matrix and then reconstruct the TFT-LCD image under inspection. Lee and Yoo (2004) developed an automatic detection method based on the modified regression diagnostics and Niblack's thresholding to filter

[†] : Corresponding Author

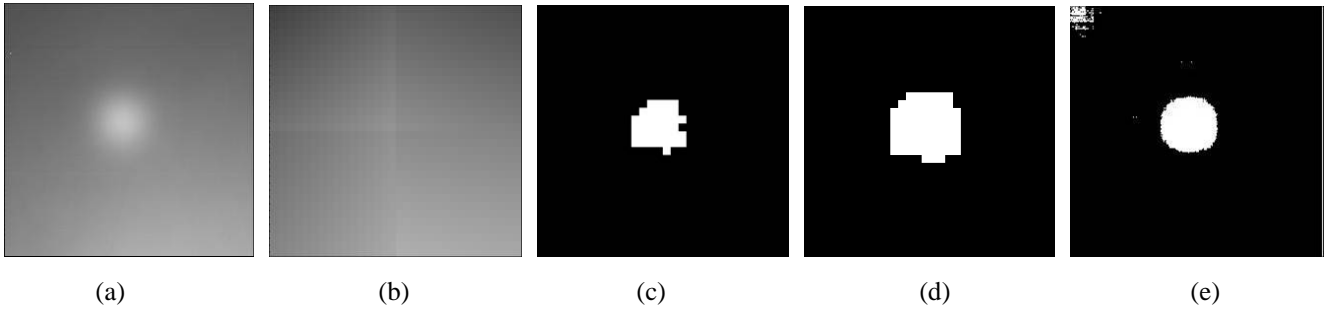


Figure 2: Computational results of each step. (a) Original image. (b) Estimated image. (c) Outlier region image. (d) Mura region dilation. (e) Mura image.

out mura pixels in TFT-LCD image. Then, the candidate Mura defects are quantified to identify real Muras. Wang and Ma (2006) proposed a recursive surface fitting model to reconstruct the non-Mura images, and computational results returned by using their method demonstrate good performance in efficiency.

An automatic inspection method for detecting TFT-LCD Mura defects is described in this paper. The inspection image is estimated by a linear model, and then Mura regions are extracted by using regression diagnostics and a proposed threshold method. Section 2 describes the proposed Mura detection method. Section 3 presents the discussion of parameter setting and experimental results on different types of Mura defects, and the conclusion is drawn in Section 4.

2. MURA DETECTION BASED ON LINEAR REGRESSION DIAGNOSTICS

There is an overview of the proposed inspection procedure in Figure 2, and those four steps in inspection procedure are described in this section. The digital input image of each TFT-LCD panel is loaded from automatic camera. The captured image is transformed into gray-level image. Each image is divided into non-overlap windows for image estimation (Figure 2b). The windows size is $W \times H$, and each window of the input gray-level image is estimated in a sequential order without overlap. The Mura region in each window is detected (Figure 2c) by the regression diagnostic method, and then divided windows are merge into a single binary image with the original positions of the gray-level image. The single binary image is then processed by morphological region dilation (Figure 2d) ensuring that the non-Mura region contains only defect-free image. At last, Mura pixels are extracted (Figure 2e) by setting a threshold to residuals between the original image and estimated image.

The procedure of the proposed Mura inspection method is outlined as follows:

1. The estimated image is constructed by a linear regression model in each window image (see Figure 3). Studentized residual of regression diagnostics is calculated from the estimated and original gray-level images. The Mura regions are screened by the threshold value of studentized residual and then merged into a single binary image.

2. The Mura regions in the merged binary image are extended by processing morphological region dilation to ensure that the non-Mura regions contain no Mura pixels.

3. Based on the merged binary image obtained from step2, the mean and standard deviation of non-Mura region residuals (between the estimated and original gray-level images) is calculated. Finally, Mura pixels are extracted by setting a threshold to residuals over all pixels in the original image. The threshold is computed based on the mean and standard deviation of residuals.

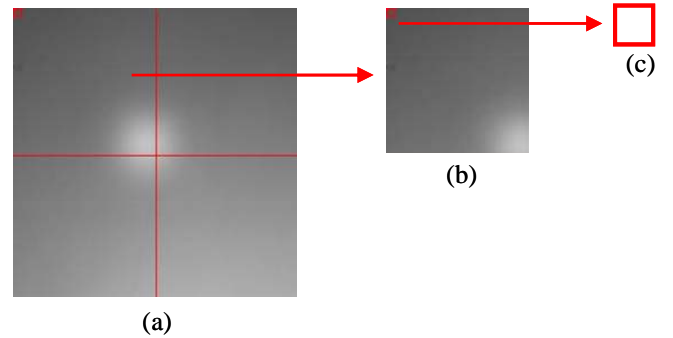


Figure 3: Illustration of non-overlapping windows and sample regions. (a) Input image. (b) non-overlapping windows. (c) Sample region.

2.1 Construction of Estimated Image

The first step is to construct the estimated image by a linear regression model. In the linear model, x_1 represents the position of the pixel in the x axis, x_2 represents the position of the pixel in the y axis, and y is

the gray-level value of the pixel on position (x_1, x_2) .

$$y = f(x_1, x_2),$$

$$x_1 = x_{pos} \quad x_2 = y_{pos} \cdot$$

Thus, the equation of the linear model is

$$y = \beta_0 + \beta_1 x_1 + \beta_2 x_2 + \mathcal{E},$$

where \mathcal{E} is the error term. To use the linear regression model to calculate the residuals of the image's gray level values, the hat matrix \mathbf{H} can be first computed, as given by

$$\mathbf{H} = \mathbf{X}(\mathbf{X}^T \mathbf{X})^{-1} \mathbf{X}^T$$

where \mathbf{X} in the linear model is equal to $[\mathbf{1}, \mathbf{x}_1, \mathbf{x}_2]$. The hat matrix has several useful properties. It's symmetric ($\mathbf{H}^T = \mathbf{H}$) and idempotent ($\mathbf{H}\mathbf{H} = \mathbf{H}$). Similarly, the matrix $\mathbf{I} - \mathbf{H}$ is also symmetric and idempotent. The estimated image is $\hat{\mathbf{y}} = \mathbf{H}\mathbf{y}$. The hat matrix \mathbf{H} can be directly computed without having to explicitly construct the entire regression model, thus making the image estimation procedure very efficient. It can be deemed as a stationary matrix when the image to be estimated has same window size.

The original image is divided into non-overlapping windows for local processing, and then each window is estimated in order. Every parts of the estimated image are combined to one estimated gray-level image. For the sake of computation efficiency and noise reduction, the original image is estimated by sample regions instead of going over all pixels. The sample is a square region with no overlapping as illustrated in Figure 3. The local coordinate system \mathbf{X} is defined as follows:

$$(1, x_1, x_2) = (1, i, j),$$

$$i \in [0, 1, 2, \dots, W/W_{sr}], j \in [0, 1, 2, \dots, H/H_{sr}]$$

where W , H , W_{sr} and H_{sr} are heights and widths of windows for local processing and sample regions for image estimation. Each mean gray-level value of the sample region is treated as a sample point for the estimation of each window of the image. Afterwards, all pixels in each sample region share the same gray-level value estimate.

2.2 Outlier Region Detection

To filter out the Mura region in the estimated image, the second step is to conduct regression diagnostics. The studentized residuals are used for detecting the outlier region. The vector of residuals \mathbf{e} is the difference of $\hat{\mathbf{y}}$ and \mathbf{y} , which is defined by

$$\hat{\mathbf{y}} = \mathbf{H}\mathbf{y}, \quad \mathbf{e} = (\mathbf{I} - \mathbf{H})\mathbf{y}$$

The studentized residuals r_i is

$$r_i = \frac{e_i}{\sqrt{MSE(1 - h_{ii})}}, \quad i = 1, 2, \dots, \text{num_sample},$$

where e_i is the i th element in the vector of residuals, MSE is the mean square error of the vector of residuals, and h_{ii} is the i th diagonal element of the hat matrix (Montgomery and Peck 1992). The decision rule is that if the absolute value of studentized residuals is greater than the threshold, then that sample region is earmarked as an outlier region (Figure 2c).

2.3 Mura Region Dilation

There is an extra image manipulation necessary for the outlier region where the method adopted is the 8-neighbor region dilation. This idea is inspired by dilation in mathematical morphology (Gonzalez and Woodes 2002). When a region is considered an outlier region, its 8-neighbor regions are also set to be outliers. This manipulation tries to cover as much the Mura area as possible. In doing so, the remaining area contains almost purely non-Mura pixels, thus making MSE a more accurate estimate of the variance of the defect-free gray-level values.

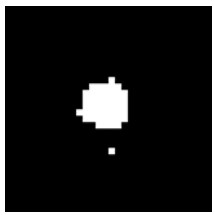
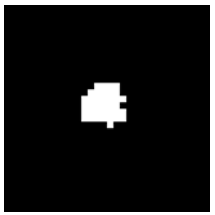
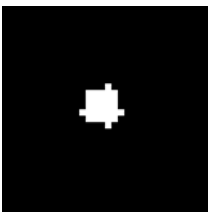
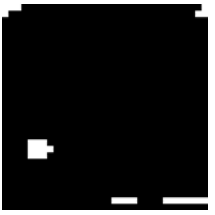
2.4 Mura Pixel Detection

The last step is to decide on a threshold for filtering Mura pixels. The idea of the threshold is inspired from statistical process control (SPC) in quality control (QC), and the threshold is set equal to $\mu + n * \sigma$, where n is the constant to be pre-specified by the user. The mean and the standard deviation are calculated based upon all difference gray-level values of non-Mura pixels between the original and estimated images (i.e., residuals). There is only the upper bound to filter the Mura image since the minimum value of the difference expects to be zero. Subsequently, the differences of all the gray-level values (of both Mura and non-Mura pixels) between original and estimated images are filtered by the proposed threshold. If the difference is greater than the threshold, the pixel is set to be a Mura pixel.

3. EXPERIMENTAL RESULTS

In this section, the parameter setting is discussed and then experimental results of detecting Mura images by using the proposed method are presented. The original image (256×256) is divided into 4 windows (128×128), and then each window is estimated in order. The sample region size of each window is 8×8 without overlapping. The sample mean of gray-level values of all pixels in the 8×8 image is treated as one sample point for image

Table 1: Outlier region images of using different thresholds for studentized residuals.

Original image	Threshold = 1.5	Threshold = 2.0	Threshold = 2.5
			
			
			

estimation. In this paper, two scenarios of experimental results are considered. The first scenario is to set the different threshold values for the studentized residuals. The second scenario is to set different parameter n for the threshold in the Mura pixel detection on normal and Mura images. Normal images present the normal input image without Mura defects. However, the images are sometimes examined under non-uniform illumination conditions, which will much complicate the inspection of Mura defects and then mislead the proposed method to yield incorrect results. The two above-mentioned parameter settings in these two scenarios are used to investigate the sensitivity of the proposed method under different illumination conditions.

3.1 Different Threshold for Outlier Region Detection

To detect Mura regions between the estimated and original images, the studentized residuals are calculated for each sample region. When the studentized residual is greater than the threshold, the sample region corresponding to that studentized residual will be treated as outlier region. The threshold is set to 1.5, 2.0 and 2.5 for evaluating the sensitivity of proposed method in the first scenario. The resulting images of each step are displayed in Table 1.

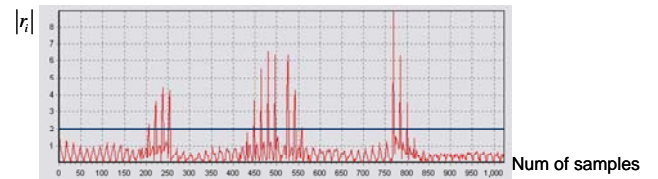


Figure 4: the studentized residuals and the threshold

As the threshold is set equal to 1.5, the outlier regions contain many misclassified regions. When the threshold is set equal to 2.5, the outlier region is a bit smaller than the actual area of the Mura region. Therefore, setting the threshold to 2.0 in the first scenario is recommended.

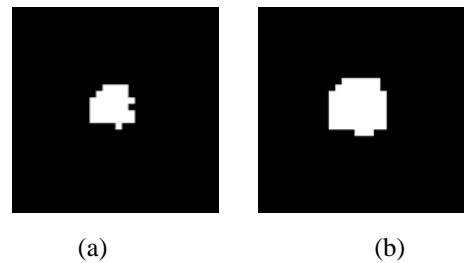
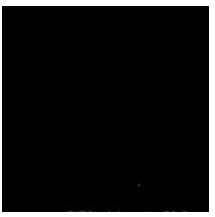
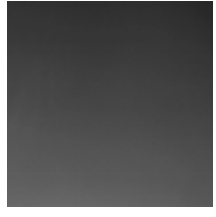
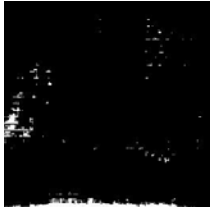
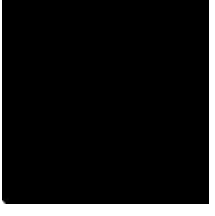


Figure 5: Illustration of 8-neighbor region dilation. (a) Outlier region image. (b) Resulting image after 8-neighbor region dilation.

Table 2: Resulting images for setting different parameter n for Mura pixel detection.

Original image	$n = 2.5$	$n = 3.0$	$n = 3.5$
			
			
			

3.2 Different Parameter Settings on the Threshold for Mura Pixel Detection

After filtering out the outlier region, the outlier region image is extended by processing the 8-neighbor region dilation. In Figure 5, the resulting image represents the outlier region image after applying 8-neighbor region dilation. This method attempts to ensure that all potential Mura pixels are covered by the Mura regions (white regions in Figure 5). The second scenario is to set different parameter n to the threshold for Mura pixel detection on the normal and Mura images. The parameter n is set to 2.5, 3.0 and 3.5 for the comparison purpose. Table 2 lists the resulting images for different parameter n on normal images. First, the normal image (without Mura defects) is examined, and the best result is that there is no Mura pixel found. The best result is obtained when n is set equal to 3.5. When parameter n is set to 2.5 and 3.0, the output will be affected by non-uniform illumination and generate unnecessary noises. While detecting the Mura images (see Appendix A1), the threshold parameter being set to 3.5 could produce better results with less misclassified pixels than the other two settings. Under this setting, the proposed method could detect the spot and line Mura effectively, but fail in detecting the ring with threshold parameter of 3.5. As evidenced by Appendix A1, the threshold parameter of 2.5

or even smaller is suggested to increase the detection sensitivity for the ring Mura case. The proposed method is coded by Borland C++ Builder 6.0. In general, it takes about half a second for image estimation and outlier region detection and 0.8 second for Mura pixel detection. Test images are tested under Intel Core 2 Duo-2.66GHz platform with 2 GB DDR SDRAM on the WinXP system.

4. CONCLUSIONS AND FUTHER RESEARCH

This paper has presented a Mura detection method that is based on regression diagnostics using studentized residuals for automatic Mura inspection of FPD, and the experimental results show that the proposed method is effective and efficient. The estimated image is constructed by the linear regression model for calculating studentized residuals, and Mura regions and Mura pixels are extracted by two proposed threshold methods. As a practical guidance, the suggested threshold value for the studentized residuals is 2.0, and 3.5 for the Mura pixel detection to achieve robust inspection outcomes. For further research, large-scale industrial images and other Mura types should be included to further validate the effectiveness of the proposed method. Alternative regression diagnostics particularly designed for ring Mura defects deserve a future study.

APPENDIX

A1: Result images for different parameter n on Mura images.

Mura Type	Original image	$n = 2.5$	$n = 3.0$	$n = 3.5$
Spot				
Spot				
Line				
Line				
Ring				

REFERENCES

Gonzalez, R. C., and Woodes, R. E. (2002) *Digital image Processing*, 2nd edition, Prentice Hall.

Lee, J. Y., and Yoo, S. I. (2004) Automatic detection of region-mura defect in TFT-LCD. *IEICE Transactions on Information and Systems*, **E87-D**, no. 10, 2371-2378.

Lu, C. J., and Tsai, D. M. (2005) Automatic Defect Inspection for LCDs Using Singular Value Decomposition. *The International Journal of Advanced Manufacturing Technology*, **25**, 53-61.

Lu, C. J., and Tsai, D. M. (2008) Independent component analysis-based defect detection in patterned liquid crystal display surfaces. *Image and Vision Computing*, **26**, 955-970

Montgomery, D. C., and Peck, E. A. (1992) *Introduction to Linear Regression Analysis*, 2nd edition, Wiley-Interscience.

Pratt, W. K., Sawkar S. S., O'reilly, K. (1998) Automatic blemish detection in liquid crystal flat panel displays. *IS&T/SPIE Symposium on electronic imaging: Science and Technology*, 3306, San Jose, California.

VESA Flat Panel Display Measurements Standard Ver. 2.0 (2001)

Wang, Z. Y., and Ma, L. (2006) Implementation of region-mura detection based on recursive polynomial-surface fitting algorithm. *Proceedings of the 2nd Asia International Symposium on Mechatronics, Hong Kong, China*, 1-6.

AUTHOR BIOGRAPHIES

Yu-Chiang Chuang is currently a Ph.D. student in industrial engineering and management at Yuan Ze University, Taiwan, ROC. His research interests include meta-heuristic, image processing, image registration and computational intelligence. His email address is <jack@r2r.iem.yzu.edu.tw>

Shu-Kai S. Fan is a professor of industrial engineering and management at Yuan Ze University, Taiwan, ROC. He received his bachelor degree in Industrial Engineering from Tung hai University, master degree in Industrial Engineering from University of Pittsburgh and doctor degree in industrial engineering from the University of Texas at Arlington (UTA). His research interests include areas of applied statistics, applied mathematical programming, response surface optimization, advanced process control and particle swarm optimization. His email address is <simonfan@saturn.yzu.edu.tw>